Variable-Temperature Kinetic Analysis of a Three-Site Terminal Ligand Exchange in Nickel A-Frames by Quantitative $^{31}P\{^1H\}$ EXSY NMR

Jerald D. Heise, Daniel Raftery,* Brian K. Breedlove, John Washington, and Clifford P. Kubiak*,†

Department of Chemistry, Purdue University, 1393 Brown Laboratory of Chemistry, West Lafayette, Indiana 47907-1393

Received July 2, 1998

Variable-temperature two-dimensional phase-sensitive $^{31}P\{^1H\}$ EXSY NMR spectroscopy was used to determine the kinetics and thermodynamics of terminal ligand redistribution in the nickel A-frames $Ni_2(dppm)_2(C{=}CH_2)X_2$ (X = SCN (**1**), Cl (**3**); dppm = bis(diphenylphosphino)methane). Solutions containing 1:1 mixtures of **1** and **3** undergo terminal ligand exchange via a two-step process involving a mixed-ligand intermediate, $Ni_2(dppm)_2(C{=}CH_2)$-(Cl)(SCN) (**2**). This type of terminal ligand exchange is characteristic of this class of compounds. One-dimensional $^{31}P\{^1H\}$ NMR spectra for the mixed-halogen or halogen/pseudohalogen species show a strong solvent dependence. The observed NMR spectra for **2** range from a broad singlet (DMSO) to a well-resolved AA′BB′ multiplet (benzene) and are dependent on the rate of ligand substitution. Rate constants for the terminal ligand exchange processes in DMSO-d_6 were calculated by three methods from the $^{31}P\{^1H\}$ EXSY NMR data. From these measurements, a complete thermodynamic characterization of this exchange process was achieved. Entropies of activation calculated from Eyring plots range from −11.4 to −19.0 cal/(K mol). This implies ordering of the system during the transition state and is consistent with an associative interchange (I_a) mechanistic model. Free energy calculations show an intrinsic thermodynamic stability associated with the mixed-ligand species **2**.

Introduction

Over the past 20 years, the chemistry of A-frame complexes has developed considerably.[1−18] Many of these complexes have been found to possess a rich and diverse chemistry, including novel reactivity[2,7,8,10−14,17,19−33] and catalytic activity.[11,21,34,35] Several studies of A-frame complexes have been aimed at examining the molecular dynamics of intramolecular rearrangements,[3,17,22,36−40] but intermolecular substitution reac-

† Present address: Department of Chemistry and Biochemistry, University of California, San Diego, 9500 Gilman Drive, La Jolla, CA 92093-0358.

(1) Fontaine, X. L. R.; Higgins, S. J.; Shaw, B. L.; Thorton-Pett, M.; Yichang, W. *J. Chem. Soc., Dalton Trans.* **1987**, 1501.
(2) Fontaine, X. L. R.; Higgins, S. J.; Shaw, B. L. *J. Chem. Soc., Dalton Trans.* **1988**, 1179.
(3) Manojlovic-Muir, L.; Muir, K. W.; Davis, W. M.; Mirza, H. A.; Puddephatt, R. J. *Inorg. Chem.* **1992**, *31*, 904.
(4) Heise, J. D.; Nash, J. J.; Fanwick, P. E.; Kubiak, C. P. *Organometallics* **1996**, *15*, 1690.
(5) Brown, M. P.; Fisher, J. R.; Puddephatt, R. J.; Seddon, K. R. *Inorg. Chem.* **1979**, *18*, 2808.
(6) Muralidharan, S.; Espenson, J. H. *Inorg. Chem.* **1983**, *22*, 2787.
(7) Grundy, K. R.; Robertson, K. N. *Organometallics* **1983**, *2*, 1736.
(8) Vaartstra, B. A.; O'Brien, K. N.; Eisenberg, R.; Cowie, M. *Inorg. Chem.* **1988**, *27*, 3668.
(9) Kenney, M. I. S.; Kenney, J. W., III; Crosby, G. A. *Inorg. Chem.* **1986**, *25*, 1506.
(10) Kubiak, C. P.; Eisenberg, R. *J. Am. Chem. Soc.* **1977**, *99*, 6129.
(11) Kubiak, C. P.; Eisenberg, R. *Inorg. Chem.* **1980**, *19*, 2726.
(12) Kubiak, C. P.; Woodcock, C.; Eisenberg, R. *Inorg. Chem.* **1980**, *19*, 2733.
(13) Benner, L. S.; Balch, A. L. *J. Am. Chem. Soc.* **1978**, *100*, 6099.
(14) Benner, L. S.; Olmstead, M. M.; Hope, H.; Balch, A. L. *J. Organomet. Chem.* **1978**, *153*, C31.
(15) Colton, R.; McCormick, M. J.; Pannan, C. D. *Aust. J. Chem.* **1978**, *31*, 1425.
(16) Balch, A. L.; Benner, L. S.; Olmstead, M. M. *Inorg. Chem.* **1979**, *18*, 2996.
(17) Balch, A. L.; Hunt, C. T.; Lee, C.; Olmstead, M. M.; Farr, J. P. *J. Am. Chem. Soc.* **1981**, *103*, 3764.
(18) Olmstead, M. M.; Hope, H.; Benner, L. S.; Balch, A. L. *J. Am. Chem. Soc.* **1977**, *99*, 5502.
(19) Young, S. J.; Kellenberger, B.; Reibenspies, J. H.; Himmel, S. E.; Manning, M.; Anderson, O. P.; Stille, J. K. *J. Am. Chem. Soc.* **1988**, *110*, 5744.
(20) Higgins, S. J.; Shaw, B. L. *J. Chem. Soc., Dalton Trans.* **1988**, 457.
(21) Kullberg, M. L.; Kubiak, C. P. *Organometallics* **1984**, *3*, 632.
(22) Lee, C.; Hunt, C. T.; Balch, A. L. *Organometallics* **1982**, *1*, 824.
(23) Jenkins, J. A.; Cowie, M. *Organometallics* **1992**, *11*, 2774.
(24) Jenkins, J. A.; Cowie, M. *Organometallics* **1992**, *11*, 2767.
(25) Sharp, P. R.; Ge, Y. *J. Am. Chem. Soc.* **1987**, *109*, 3796.
(26) Ge, Y.; Peng, F.; Sharp, P. R. *J. Am. Chem. Soc.* **1990**, *112*, 2632.
(27) Ge, Y.; Sharp, P. R. *J. Am. Chem. Soc.* **1990**, *112*, 3667.
(28) Vaartstra, B. A.; Xiao, J.; Jenkins, J. A.; Verhagen, R.; Cowie, M. *Organometallics* **1991**, *10*, 2708.
(29) Cameron, T. S.; Gardner, P. A.; Grundy, K. R. *J. Organomet. Chem.* **1981**, *212*, C19.
(30) Brown, M. P.; Puddephatt, R. J.; Rashidi, M.; Seddon, K. R. *J. Chem. Soc., Dalton Trans.* **1978**, 1540.
(31) Brown, M. P.; Puddephatt, R. J.; Rashidi, M.; Seddon, K. R. *J. Chem. Soc., Dalton Trans.* **1978**, 516.
(32) Azam, K. A.; Puddephatt, R. J. *J. Organomet. Chem.* **1982**, *234*, C31.
(33) Pringle, P. G.; Shaw, B. L. *J. Chem. Soc., Chem. Commun.* **1982**, 81.
(34) Kubiak, C. P.; Woodcock, C.; Eisenberg, R. *Inorg. Chem.* **1982**, *21*, 2119.
(35) Lee, C.; Hunt, C. T.; Balch, A. L. *Inorg. Chem.* **1981**, *20*, 2498.
(36) Brown, J. M.; Canning, L. R. *J. Chem. Soc., Chem. Commun.* **1983**, 460.
(37) Cowie, M.; Mague, J. T.; Sanger, A. R. *J. Am. Chem. Soc.* **1978**, *100*, 3628.
(38) Mague, J. T.; Sanger, A. R. *Inorg. Chem.* **1979**, *18*, 2060.

S0276-7333(98)00556-1 CCC: $15.00
Publication on Web 09/09/1998

tions have not been examined in detail. In the course of our studies of nickel A-frames $[Ni_2(dppm)_2(C{=}CH_2)X_2]$ (X = SCN (**1**), Cl (**3**), Br (**4**), I (**5**), OCN (**6**); dppm = bis(diphenylphosphino)methane)[1,4] and $[Ni_2(dmpm)_2(C{=}CH_2)X_2]$ (X = Cl (**7**), Br (**8**), I (**9**); dmpm = bis(dimethylphosphino)methane),[4] we observed an extremely facile intermolecular terminal ligand exchange. Solutions of $[Ni_2(diphos)_2(C{=}CH_2)(X)_2]$ and $[Ni_2(diphos)_2(C{=}CH_2)Y_2]$ (where diphos = dppm, dmpm) exist in equilibrium with the mixed-ligand species $[Ni_2(diphos)_2(C{=}CH_2)(X)(Y)]$ (X, Y = Cl, Br, I, OCN, SCN; eq 1, P atoms omitted for

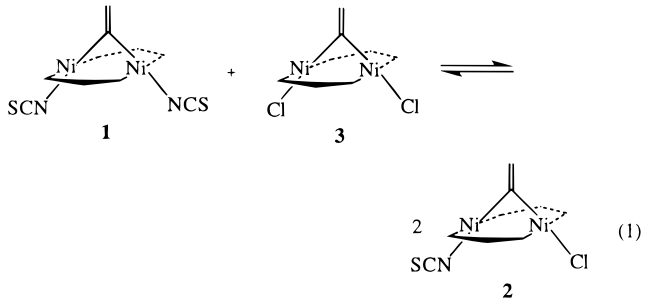

(1)

clarity). Metathesis reactions of this type are commonly referred to as redistribution reactions.[41] These reactions occur in DMSO and acetone as well as in relatively nonpolar and noncoordinating solvents such as methylene chloride and benzene. The redistribution equilibrium is rapidly established, and there is an intrinsic thermodynamic stability associated with the mixed-ligand species. The A-frame metathesis reactions discussed here can be easily followed by one- and two-dimensional ^{31}P NMR. Two-dimensional EXSY (exchange spectroscopy) NMR is a powerful technique to obtain reliable rate constants and activation parameters for systems that are in equilibrium, including isomerization[42−53] and redistribution[54,55] reactions. We report variable-temperature two-dimensional $^{31}P\{^1H\}$ EXSY NMR studies of A-frame redistribution reactions. We have determined the forward and reverse rate constants for the interconversion of **1**, **2,** and **3**. The unidirectional pseudo-first-order rate constants that represent transfer of magnetization due to chemical exchange are defined in eq 2. The activation parameters and the relative energetics were then determined in variable-temperature studies.

$$\underset{\mathbf{1}}{M_2(NCS)_2} \underset{k_{21}}{\overset{k_{12}}{\rightleftharpoons}} \underset{\mathbf{2}}{M_2(NCS)(Cl)} \underset{k_{32}}{\overset{k_{23}}{\rightleftharpoons}} \underset{\mathbf{3}}{M_2(Cl)_2} \qquad (2)$$

$$M_2 = Ni_2dppm_2(CCH_2)$$

Redistribution reactions have been studied extensively for most of the main-group elements.[41,55−62] Redistribution reactions involving transition-metal coordination compounds have not been studied extensively.[60,63−68] Murray et al. reported a qualitative observation of terminal ligand exchange for a series of gold A-frames, $[Au_2(CH_2PPh_2CH_2)(CH_2)X_2]$ (X = Cl, Br, I).[68] To our knowledge, this is the first *quantitative* study of a redistribution reaction for A-frame complexes and among the first to apply $^{31}P\{^1H\}$ 2D EXSY NMR spectroscopy to a redistribution reaction, in general.

Materials and Methods

Chemicals and Sample Preparation. NMR solvents were purchased from Aldrich or Cambridge Isotope Laboratories and were used without further purification. Compounds **1**, **3**−**5**,[1] **6**,[4] and **7**−**9**[4] were prepared according to previously reported methods. Compounds used in the two-dimensional EXSY NMR experiments were recrystallized three times from THF/hexane and dried under vacuum prior to use. NMR samples for the EXSY experiments were prepared in DMSO-d_6, and A-frames **1** and **3** were combined in a 1:1 molar ratio. Total concentrations of **1** and **3** per sample were 30.9, 26.3, 26.6, and 31.8 mM for data collected at 20, 30, 40, and 50 °C, respectively.

NMR Measurements. All $^{31}P\{^1H\}$ NMR measurements were made on a Varian XL-200 spectrometer operating at 80.997 MHz equipped with a 5 mm probe. All $^{31}P\{^1H\}$ spectra were referenced to external 85% H_3PO_4. Temperature calibration was determined using an ethylene glycol chemical shift thermometer accurate to ±0.5 °C.

The spin−lattice relaxation (T_1) times, determined by the inversion recovery method,[48] and the spin−spin relaxation (T_2) times, determined by the Carr−Purcell spin−echo method,[48] in DMSO-d_6, are reported in Table 1 and Table 2, respectively. Line widths from one-dimensional spectra (DMSO-d_6) were

(39) Deraniyagala, S. P.; Grundy, K. R. *Organometallics* **1985**, *4*, 424.
(40) Woodcock, C.; Eisenberg, R. *Inorg. Chem.* **1985**, *24*, 1285.
(41) Lockhart, J. C. *Redistribution Reactions*; Acedemic Press: New York, 1970, and references therein.
(42) Meier, B. H.; Ernst, R. R. *J. Am. Chem. Soc.* **1979**, *101*, 6441−6442.
(43) Jeener, J.; Meier, B. H.; Bachmann, P.; Ernst, R. R. *J. Chem. Phys.* **1979**, *71*, 4546.
(44) Perrin, C. L.; Gipe, R. K. *J. Am. Chem. Soc.* **1984**, *106*, 4036−4038.
(45) Ismail, A. A.; Sauriol, F.; Sedman, J.; Butler, I. S. *Organometallics* **1985**, *4*, 1914−1915.
(46) Wynants, C.; Binst, G. V.; Mugge, C.; Jurkschat, K.; Tzschach, A.; Pepermans, H.; Geilen, M.; Willem, R. *Organometallics* **1985**, *4*, 1906−1909 and references therein.
(47) Willem, R. *Prog. NMR Spectrosc.* **1987**, *20*, 1−94.
(48) Ernst, R. R.; Bodenhausen, G.; Wokaun, A. *Principles of Nuclear Magnetic Resonance in One and Two Dimensions*; Clarendon: Oxford, U.K., 1987.
(49) Ni, J.; Kubiak, C. P. *Inorg. Chem.* **1990**, *29*, 4345−4347.
(50) Perrin, C. L.; Dwyer, T. J. *Chem. Rev.* **1990**, *90*, 935−967.
(51) Willem, R.; Bieseman, M.; Hallenga, K.; Lippens, G.; Malaisse-Lagae, F.; Malaisse, W. J. *J. Biol. Chem.* **1992**, *267*, 210−217 and references therein.
(52) Kayser, F.; Biesemans, M.; Willem, R.; Malaisse-Lagae, F.; Malaisse, W. J. *Biochem. J.* **1993**, *295*, 607−609.
(53) Wang, D.; Shen, H.; Richmond, M. G.; Schwartz, M. *Organometallics* **1995**, *14*, 3636−3640.
(54) Ramachandran, R.; Knight, C. T. G.; Kirkpatrick, R. J.; Oldfield, E. *J. Magn. Reson.* **1985**, *65*, 136−141.
(55) Knight, C. T. G.; Kirkpatrick, R. J.; Oldfield, E. *J. Magn. Reson.* **1988**, *78*, 31−40.
(56) Van Wazer, J. R.; Moedritzer, K. *Angew. Chem., Int. Ed. Engl.* **1966**, *5*, 341.
(57) Moedritzer, K. *J. Organomet. Chem.* **1966**, *1*, 179.
(58) Moedritzer, K. *Advances in Organometallic Chemistry*; Academic Press: New York, 1968; Vol. 6, pp 172−271.
(59) Lockhart, J. C. *Chem. Rev.* **1965**, *65*, 131−151.
(60) Ziegler, K. *Organometallic Chemistry*; ACS Monograph; Reinhold Publishing: New York, 1960, p 194.
(61) Mole, T. *Organometallic Reactions*; Wiley-Interscience: New York, 1970; Vol. 1, pp 1−54.
(62) Moedritzer, K. *Organometallic Reactions*; Wiley-Interscience: New York, 1971; Vol. 2, pp 1−115.
(63) Weingarten, H.; Van Wazer, J. R. *J. Am. Chem. Soc.* **1966**, *88*, 2700−2702.
(64) Weingarten, H.; Van Wazer, J. R. *J. Am. Chem. Soc.* **1965**, *87*, 724−730.
(65) Heaton, B. T.; Timmons, K. J. *J. Chem. Soc., Chem. Commun.* **1973**, 931−932.
(66) Linck, R. G.; Owens, B. E.; Poli, R.; Rheingold, A. L. *Gazz. Chim. Ital.* **1991**, *121*, 163−168.
(67) Hunt, C. T.; Balch, A. L. *Inorg. Chem.* **1982**, *21*, 1641−1644.
(68) Murray, H. H.; Fackler, J. P.; Mazany, A. M. *Organometallics* **1984**, *3*, 1310.

Table 1. Spin−Lattice Relaxation (T_1) Times[a] in Seconds for 1, 2, and 3 (in DMSO-d_6)

	20 °C	30 °C	40 °C	50 °C
1	1.18	1.40	1.60	1.90
2	1.19	1.48	1.68	2.01
3	1.19	1.52	1.62	1.99

[a] Errors are ±1−5%.

Table 2. Spin−Spin Relaxation (T_2) Times[a] in Seconds for 1, 2, and 3 (in DMSO-d_6)

	20 °C	30 °C	40 °C	50 °C
1	0.094	0.043	0.028	0.014
2	0.040	0.030	0.023	0.017
3	0.125	0.062	0.044	0.026

[a] Errors are ± 1−25%.

Table 3. Calculated Spin−Spin Relaxation (T_2*) Times[a] in Seconds for 1, 2, and 3 (in DMSO-d_6)

	20 °C	30 °C	40 °C	50 °C
1	0.034	0.029	0.022	0.016
2	0.022	0.022	0.017	0.016
3	0.038	0.036	0.030	0.022

[a] Errors are ± 3−7%.

used to calculate T_2*, where $T_2^* = (\pi \times \text{line width})^{-1}$ (see Table 3). One-dimensional spectra used for integration were acquired with a recycle time of $6T_1$ and 90° pulse widths.

To investigate the salt concentration dependency, a stock solution containing equimolar (30 mmol) concentrations of **1** and **3** was prepared in a 10 mL volumetric flask in DMSO-d_6. Using a pipet, 1 mL aliquots of the stock solution were transferred to different vials. To these vials were added 0.1, 0.2, 0.3, 0.4, and 0.6 equiv of NH_4Cl and KSCN. The samples were shaken to dissolve the salt and then transferred to NMR tubes. T_2 and T_2* measurements were obtained for each sample.

Collection of the two-dimensional phase-sensitive $^{31}P\{^1H\}$ EXSY data included 32 transients per increment with a total of 128 increments. A standard phase-sensitive NOESY pulse sequence was used, preparation−90°−t_1−90°−HS−t_m−90°−acquisition, where HS = homospoil pulse. Recycle times for the EXSY pulse sequence were 4 times the measured T_1 values. Total acquisition time was approximately 15−20 h/experiment. EXSY spectra were obtained at 20 °C (t_m = 75, 100, 1500, 2000 ms), 30 °C (t_m = 0, 10, 25, 50, 100, 200, 500 ms), 40 °C (t_m = 10, 25, 50, 100 ms), and 50 °C (t_m = 0, 10, 25, 50 ms). The two-dimensional spectra were phased in both dimensions. Drift corrections were made as necessary. Standard Varian software was used to determine the auto and cross-peak volumes. Cross-peaks were normalized according to the procedure reported by Macura et al.[69] and Ramachandran et al.[54]

Only two data sets where t_m = 0.0 s were acquired. EXSY NMR experiments are very time-intensive, and samples containing mixtures of **1**, **2**, and **3** undergo some decomposition after 20 h at higher temperatures. Therefore, each sample was prepared to the same specifications with 1:1 ratios of **1** and **3** (ca. 30 mM). Peak volumes from the EXSY spectra where t_m = 0 are needed in order to utilize method A and method B (vide infra). Since the peak areas of a one-dimensional experiment and the peak volumes of a two-dimensional experiment (where t_m = 0) should be directly related, the two-dimensional peak volumes were calculated by scaling the one-dimensional areas for experiments in which t_m = 0 data were not obtained. One-dimensional areas (mole fractions) can be used to normalize the cross-peak intensities in method C (vide infra).[51]

(69) Macura, S.; Farmer, B. T., III; Brown, L. R. *J. Magn. Reson.* **1986**, *70*, 493−499.

Table 4. Integrated Areas for One-Dimensional Spectra and Volumes for Two-Dimensional (t_m = 0.0 s) Spectra at Different Temperatures

	1	**2**	**3**
		20 °C	
1D area	0.217	0.575	0.209
		30 °C	
1D area	0.219	0.578	0.203
2D vol	3.29×10^{-4}	8.68×10^{-4}	3.44×10^{-4}
		40 °C	
1D area	0.203	0.562	0.235
		50 °C	
1D area	0.199	0.570	0.231
2D vol	2.56×10^{-4}	8.98×10^{-4}	3.94×10^{-4}

Selection of Data at Appropriate Mixing Times. Mixing times must be selected to maximize signal-to-noise in the cross-peaks. However, long mixing times show T_1 relaxation effects which result in large errors in the calculated rates of exchange.[69] Optimal mixing times can by approximated by eq 3, where $t_{m(opt)}$ is the optimal mixing time, T_1 is the spin−

$$t_{m(opt)} \approx \frac{1}{T_1^{-1} + k_{ij} + k_{ji}} \qquad (3)$$

lattice relaxation, and k_{ij} and k_{ji} are the exchange rates from site i to j and j to i, respectively.[50] These approximations were taken into consideration when determining the reliability of the calculated rates for methods A−C.

Activation Parameters. The activation parameters were calculated using the Eyring equation (4) by plotting $\ln(k_{ij}/T)$ vs $1/T$, where the slope and intercept of the plot were used to determine $\Delta H^‡$ and $\Delta S^‡$, respectively. The transmission coefficient (κ) was set equal to 1.

$$\ln(k_{ij}/T) = -\Delta H^‡/RT + \Delta S^‡/R + \ln(\kappa k_b/h) \qquad (4)$$

Results and Discussion

Terminal Ligand Exchange between d^8−d^8 Nickel A-Frames. One-Dimensional Spectra. For $[Ni_2(dppm)_2(C{=}CH_2)X_2]$ (X = NCS (**1**), Cl (**3**)) only two sites are available for substitution. There is one intermediate product, $[Ni_2(dppm)_2(C{=}CH_2)(Cl)(NCS)]$ (**2**), resulting from terminal ligand metathesis. For all examples discussed, equilibria were established by the time the samples were prepared and taken to the spectrometer. In every case, three species (**1**, **2**, and **3**) were observed by $^{31}P\{^1H\}$ NMR. The samples were allowed to sit undisturbed at ambient temperatures for 24−48 h, and no changes in the integrated areas of the peaks were observed. Table 4 lists the relative mole fractions of **1**, **2**, and **3** from the one-dimensional spectra. One-dimensional $^{31}P\{^1H\}$ NMR spectra of 1:1 mixtures of **1** and **3** in various solvents are shown in Figure 1. In each case, there are singlets that correspond to **1** (∼23.5 ppm) and **3** (∼19.5 ppm) along with a second-order pattern (Figure 1b,c) centered at ∼21.3 ppm. The well-resolved AA′BB′ pattern in methylene chloride and benzene collapses to a broad singlet in DMSO. The AA′BB′ spectrum is assigned to the mixed-ligand compound **2**. The complexity of the $^{31}P\{^1H\}$ NMR pattern exhibited by **2** is highly dependent on the polarity of the solvent. The transformation of the AA′BB′ pattern to a broad singlet is attributed to a combination of exchange line broadening and unresolved coupling, where the relative rates of exchange in different solvents are DMSO-d_6 >

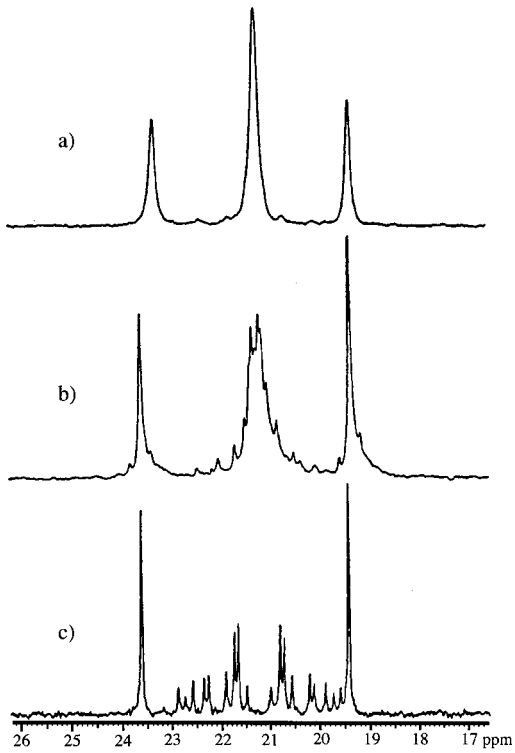

Figure 1. Solvent-dependent $^{31}P\{^1H\}$ NMR spectra of $Ni_2dppm_2(C{=}CH_2)(SCN)_2$ (**1**) and $Ni_2dppm_2(C{=}CH_2)Cl_2$ (**3**) in equilibrium with the mixed-ligand species $Ni_2dppm_2(C{=}CH_2)(NCS)Cl$ (**2**) in DMSO-d_6 (a), CD_2Cl_2 (b), and C_6D_6 (c).

$CD_2Cl_2 \gg C_6D_6$. The effects of line broadening can also be seen by comparing the differences in the T_2 (homogeneous contribution) and T_2* values (Tables 2 and 3, respectively). In some instances, T_2* is 50−60% shorter than the T_2 values in DMSO-d_6. Spin−lattice (T_1) relaxation rates were determined for species **1**, **2**, and **3** in DMSO-d_6 and are shown in Table 1. Spin−lattice relaxation rates were found to increase with temperature, which is attributed to a decrease in correlation time.

The effect of the free ligand concentration on the rate of exchange was explored. Different concentrations of the ligands NCS^- and Cl^- were added to samples of a stock solution containing both **1** and **3**. No significant changes in T_2* and T_2 were observed for the different concentrations in the range from 3 to 18 mmol, indicating that these concentrations of the free ligand have little effect on the exchange process in a polar solvent such as DMSO-d_6.

Two-Dimensional EXSY Spectra. Two-dimensional EXSY NMR experiments were acquired at various temperatures with different mixing times. The EXSY NMR experiments required 15−20 h/data set, and at 30 °C seven data sets/sample were obtained. Due to the difficulty in maintaining homogeneous solutions in some solvents for long periods of time, rate constants were calculated for reactions in DMSO-d_6 only. The equilibrium mole fractions of **1**, **2,** and **3** from the two-dimensional (where $t_m = 0$) spectra at 30 and 50 °C are reported in Table 4. A typical $^{31}P\{^1H\}$ two-dimensional EXSY phase-sensitive contour map obtained at 30 °C and 80.997 MHz with a mixing time of 25 ms is shown in Figure 2a. The three resonances appearing along the

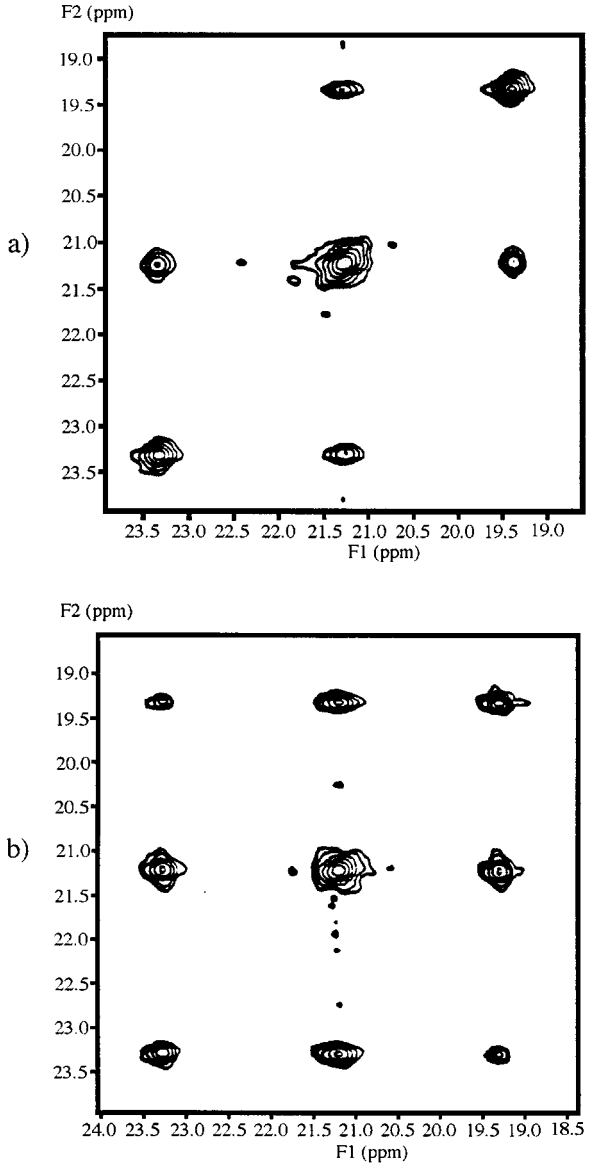

Figure 2. Contour maps of two-dimensional phase-sensitive $^{31}P\{^1H\}$ EXSY NMR (80.997 MHz) at 30 °C: (a) t_m = 25 ms; (b) t_m = 100 ms. The three resonances on the diagonal arise from the presence of $Ni_2dppm_2(C{=}CH_2)(SCN)_2$ (**1**), $Ni_2dppm_2(C{=}CH_2)NCSCl$ (**2**), and $Ni_2dppm_2(C{=}CH_2)Cl_2$ (**3**) at 23.3, 21.3, and 19.4 ppm, respectively.

diagonal at 23.3, 21.3, and 19.4 ppm correspond to **1**, **2,** and **3**, respectively, and show chemical exchange cross-peaks. Figure 2a shows cross-peaks with strong intensities that correlate the single-step interconversions of **1** to **2** and of **2** to **3**. Cross-peaks that correlate single-step interconversion are of high intensity, usually on the same order of magnitude as the diagonal peaks. At longer mixing times (100 ms), cross-peaks that correlate the two-step interconversion of **1** to **3** appear (Figure 2b). The intensities of the two-step cross-peaks are usually 2 orders of magnitude smaller than the diagonal peaks. Spectra recorded at higher temperatures (i.e. 50 °C), where exchange rates are substantially faster, show cross-peaks that correlate the interconversion of **1** and **3** at mixing times as short as 25 ms.

Double exchange, **1** to **3**, is not observed in the exchange buildup curves when mixing times are sufficiently small. Figure 3 shows a typical buildup curve

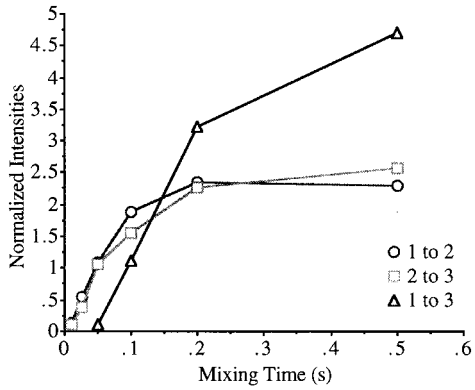

Figure 3. Buildup curves (method A) of the normalized cross-peak intensities vs mixing time (in seconds) from a phase-sensitive $^{31}P\{^1H\}$ EXSY NMR (80.997 MHz) at 30 °C.

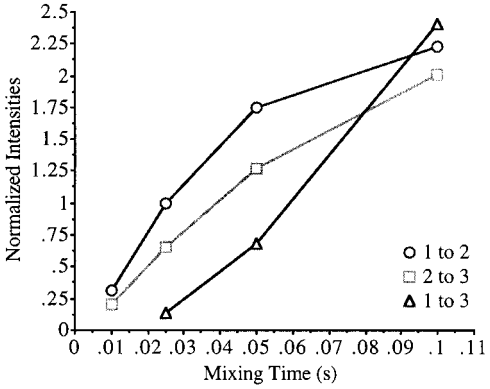

Figure 4. Buildup curves (method A) of the normalized cross-peak intensities vs mixing time (in seconds) from a phase-sensitive $^{31}P\{^1H\}$ EXSY NMR (80.997 MHz) at 40 °C.

resulting from six experiments at 30 °C. The exchange of **1** to **2** and of **2** to **3** reaches the T_1 limited maximum around 500 ms. At longer mixing times, the exchange buildup curves start to decrease. Note that the appearance of the exchange of **1** to **3** has an induction period and just begins to appear at 50 ms (Figure 3). This is characteristic of multistep exchange pathways.[51] Figure 4 is a buildup curve resulting from four experiments at 40 °C where the mixing times were 10, 25, 50, and 100 ms. The interconversion of **1** and **3** shows initially a zero slope with a strong inflection at longer mixing times. This type of inflection is also characteristic of multistep exchange processes.[51] Therefore, the conversion of **1** to **3** is assigned to two sequential one-step processes.

Evaluating Rate Constants from 2D-EXSY Spectra. EXSY spectroscopy has been widely used to give reliable rate constants for chemical exchange.[42−55] Various methods for calculating rate constants from two-dimensional EXSY spectra have been discussed in detail by Perrin and Dwyer.[50]

Three methods presented here as A, B, and C were used to determine rate constants from the 2D-EXSY spectra. All three of these methods are based on eq 5,

$$\mathbf{I}_{ij}(t_m) = (e^{-\mathbf{R}t_m})_{ij}\mathbf{M}_j^\circ \qquad (5)$$

which relates the cross-peak intensities $\mathbf{I}_{ij}$ (where i and j take values from 1 to 3) at mixing time t_m to the rate matrix $\mathbf{R}$[44,70] and the bulk magnetization vector $\mathbf{M}_j^\circ$ ($t_m = 0$). For our calculations, the matrix was symmetrized by replacing each I_{ij} value by $(I_{ij} + I_{ji})/2$. The matrix $\mathbf{R}$ contains the rate constants k_{ij} and the spin−lattice relaxation rates $R_{1(i)}$. The additive term Δ, in the diagonal, is a proportionality constant which relates the mole fraction n_i to the M_j° values.[50,53]

$$\mathbf{R} = \begin{pmatrix} -R_{1(1)} - k_{12} - k_{13} + \Delta & k_{21} & k_{31} \\ k_{12} & -R_{1(2)} - k_{21} - k_{23} + \Delta & k_{32} \\ k_{13} & k_{23} & -R_{1(3)} - k_{31} - k_{32} + \Delta \end{pmatrix}$$

Method A. An initial rate approach can be used; however, it is only valid at short mixing times, where T_1 relaxation is minimized and buildup curves are linear and increasing.[47,50,51,54,70] To determine these conditions, the normalized cross-peak volumes are plotted with respect to the mixing times.[69] The normalized cross-peak volume (I_n) is represented as

$$I_n(t_m) = \frac{I_{ij}(t_m)}{0.5n_j d_{ii}(t_m) + 0.5n_i d_{jj}(t_m)} \qquad (6)$$

where $I_{ij}(t_m)$ is the average integrated cross-peak volume, d_{ii} and d_{jj} are the diagonal-peak volumes, and n_j and n_i are the experimentally measured mole fractions. Plots of this type are shown in Figures 4 and 5. Rate constants can be approximated under these conditions by restricting the expansion of Equation 5 to the linear term shown in eq 7, where I_{ij} is the integrated cross-

$$I_{ij}(t_m) \approx k_{ji}t_m M_j^\circ \quad i \neq j \qquad (7)$$

peak volume, M_j° is the corresponding equilibrium magnetization (from a 2D-EXSY experiment where $t_m = 0$), and k_{ji} is the unidirectional pseudo-first-order rate constant from site j to i.

Method A treats each rate constant as an isolated event. Therefore, the rates calculated from method A are valid only at short mixing times. At longer mixing times, calculated rates drop off by factors of 2 and in some cases, factors of 10. Thus, reliable rate constants were determined by using eq 3 and plots based on eq 6 to predict the optimal mixing times.

Method B. The approach utilized by Oldfield et al. involves plotting the normalized cross-peak intensity data as a function of I_{ij}/M°_j vs t_m.[54] Rate constants can then be directly determined by evaluating the initial slope of the curve. This is illustrated in Figure 5, which represents a plot of I_{ij}/M°_j vs t_m at 30 °C. Since the calculated rate constants depend on the slope of the buildup curves, it is imperative to select data at sufficiently short mixing times to measure the initial rates. Obviously, rates will quickly drop off as the slope decreases. An advantage of method B over method A results from an averaging of the data obtained from the

(70) Macura, S.; Ernst, R. R. *Mol. Phys.* **1980**, *41*, 95−117.

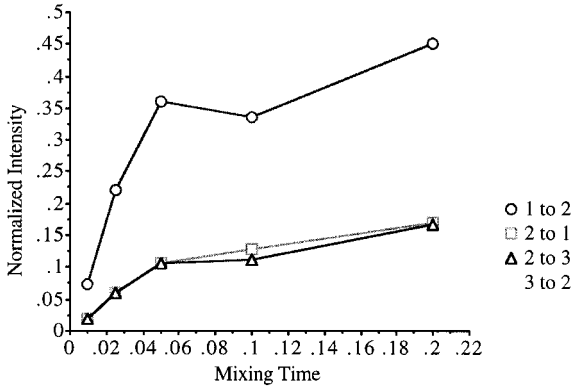

Figure 5. Buildup curves (Method B) of the normalized cross-peak intensities vs mixing time (in seconds) from a phase-sensitive $^{31}P\{^1H\}$ EXSY NMR (80.997 MHz) at 30 °C.

Table 5. Pseudo-First-Order Rate Constants (in s^{-1}) Calculated by Methods A, B, and C from Equilibrium Concentrations of 1, 2, and 3 in DMSO at 20, 30, 40, and 50 °C[a]

	20 °C	30 °C	40 °C	50 °C
		Method A		
k_{12}	5.8	8.5	15	31
k_{21}	2.2	3.4	5.4	8.9
k_{23}	1.6	2.4	4.7	8.5
k_{32}	4.4	6.3	11	19
		Method B		
k_{12}	5.6	9.0	15	31
k_{21}	2.1	3.4	5.4	8.9
k_{23}	1.5	2.2	4.7	8.5
k_{32}	4.3	6.1	11	20
		Method C		
k_{12}	6.3	13	25	51
k_{21}	2.4	5.3	9.0	15
k_{23}	1.6	3.6	6.9	13
k_{32}	4.4	9.3	17	29

[a] Errors are ±4−7%.

initial slope of the exchange buildup curve rather than a single point. In our case, the rate constants for methods A and B were similar (see Table 5).

Method C. The approach of Perrin[44,50,51] (eq 5) is to diagonalize the rate matrix **R**, using all of the peak volume data to explicitly determine forward and reverse rate constants simultaneously.[24,25,29] Method C is clearly superior to methods A and B. There are four unidirectional pseudo-first-order rate constants needed to describe this system (eq 2). Rate constants k_{12}, k_{21}, k_{23}, and k_{32} are for single-ligand exchange. The rate constants calculated by methods A, B, and C for an equilibrium mixture of **1**, **2,** and **3** in DMSO-d_6 at various temperatures are tabulated in Table 5.

In general, the errors associated with the rate constants with all three methods are low. There is also good agreement of the rate constants calculated by all three methods. At higher temperatures method C deviates from methods A and B, but two consistent trends in the data are apparent for all three methods. First, the rate constants double for every 10° increment of temperature. Second, interconversion between **1** and **2** is faster than interconversion between **2** and **3**, although at higher temperature this difference is less noticeable.

Table 6. Exchange Rates (in mol L^{-1} s^{-1} × 10^{-2}) Calculated by Methods A, B, and C (Exchange Rate = $k_{ij}[i]$) from Equilibrium Concentrations of 1, 2, and 3 in DMSO at 20, 30, 40, and 50 °C

	20 °C	30 °C	40 °C	50 °C
		Method A		
k_{12}[**1**]	3.9	4.9	8.1	20
k_{21}[**2**]	3.9	5.2	8.1	16
k_{23}[**2**]	2.9	3.7	7.1	15
k_{32}[**3**]	2.8	3.4	6.9	14
		Method B		
k_{12}[**1**]	3.8	5.2	8.1	20
k_{21}[**2**]	3.7	5.2	8.1	16
k_{23}[**2**]	2.7	3.3	7.1	15
k_{32}[**3**]	2.8	3.3	6.9	15
		Method C		
k_{12}[**1**]	4.2	7.5	14	32
k_{21}[**2**]	4.3	8.1	14	27
k_{23}[**2**]	2.8	5.5	10	24
k_{32}[**3**]	2.8	5.0	11	21

[a] Errors are ±10−14%.

Table 7. Equilibrium Constants and $\Delta G°$ Values for the Reaction of 1 and 3 in Various Solvents at 25 °C[a]

solvent	K_{eq}[b]	$\Delta G°$, kcal/mol
C_6D_6	9.22	−1.31
CD_2Cl_2	7.98	−1.22
$(CD_3)_2CO$	9.45	−1.33
DMSO-d_6	6.95	−1.15

[a] Integrations were obtained where the recycle time was $6T_1$ and pulse widths were optimized. [b] $K_{eq} = [\mathbf{2}]^2/[\mathbf{1}][\mathbf{3}]$. [c] $\Delta G° = -RT \ln(K_{eq})$. Errors in $\Delta G°$ are ±0.15 kcal.

The exchange rates can be calculated by multiplying the unidirectional pseudo-first-order rate constants by the appropriate concentration of the reacting species: i.e., exchange rate = $k_{ij}[i]$, where $[i]$ = nickel A-frame concentration of the ith species.[54] The forward and reverse exchange rates were calculated and are shown in Table 6. Clearly, the data support the equilibrium constraint that the forward and reverse rates are equal, within experimental error.

Thermodynamics. Equilibrium constants (K_{eq}) were calculated by integrating the $^{31}P\{^1H\}$ NMR spectra for mixtures of **1** and **3** in various solvents at 25 °C. Values for $\Delta G°$ are favorable and range from −1.15 to −1.33 kcal/mol; they are shown in Table 7. Equilibrium constants for the reaction shown in eq 1 ranged from 6.95 to 9.45. A relative ratio of 1:2:1 for complexes **1**, **2** and **3**, respectively, would be expected for a purely random distribution, governed by entropic effects.[58] The equilibrium constant calculated for a random distribution is $K_{rand} = 4$. Using the approach of Linck et al., the enthalpy ($\Delta H°$) of eq 1 can be approximated by assuming that the deviation of K_{eq} from K_{rand} is enthalpically driven.[66] The entropy of the reaction for the purely random redistribution is $\Delta S° = R \ln(4) = 2.8$ cal/(K mol), and thus after the entropic correction $\Delta H°$ is ∼0.3 kcal/mol for the A-frame system. This is comparable to a report of Linck et al., where they calculate a $\Delta H°$ value of ∼0.7 kcal/mol for the redistribution of $MoCp(Cl)_2(PMe_3)_2$ and $MoCp(I)_2(PMe_3)_2$ to $MoCp(Cl)I(PMe_3)_2$.[66] These values are 2 times larger than the expected value for a purely random redistribution and indicate that the exchange is not thermoneutral and ΔG

Scheme 1. Proposed Reaction Mechanism for the Conversion of 1 to 2[a]

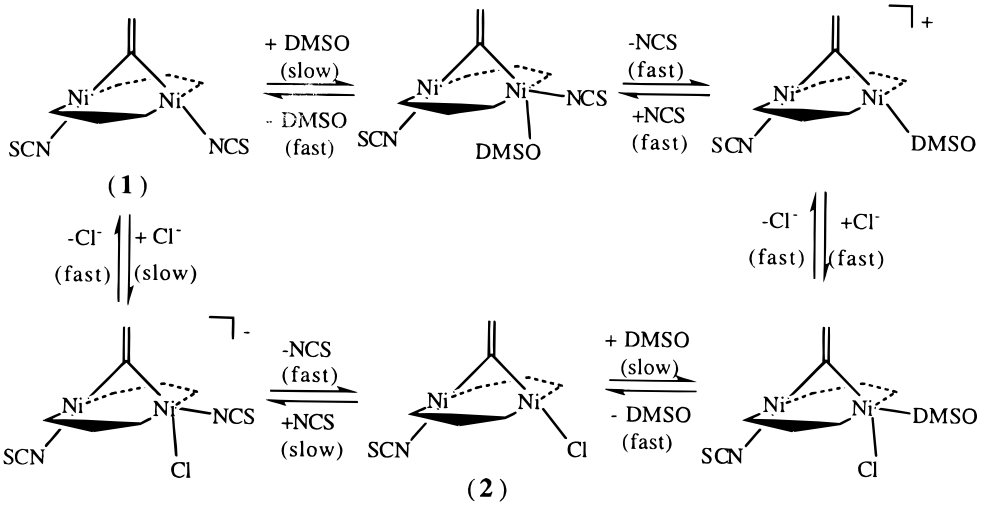

[a] P atoms omitted for clarity.

Table 8. Activation Parameters for the Redistribution of 1, 2, and 3 in DMSO-d_6[a]

			$\Delta G^{\ddagger}$ (kcal/mol)			
	$\Delta H^{\ddagger}$ (kcal/mol)	$\Delta S^{\ddagger}$ (eu)	293 K	303 K	313 K	323 K
1 to **2**	12.7	−11.4	16.1	16.2	16.3	16.4
2 to **1**	12.8	−14.0	16.8	17.0	17.1	17.3
2 to **3**	11.0	−19.0	16.6	16.8	17.0	17.2
3 to **2**	11.5	−16.4	16.3	16.4	16.6	16.8

[a] Errors are estimated at ±10−15%.

is not solely dictated by $-T\Delta S$.[59] Deviations from random distributions have been attributed to electrostatic effects where the equilibrium constant (K_{eq}) expressed as $\log K_{eq} = \log K_{stat} + \log K_{el} + \log K_R$ ($K_{stat} = K_{rand}$, K_{el} = stabilization of the mixed complex due to electrostatic effects, K_R = any additional stabilization).[59,71] In a similar system studied by Hunt and Balch, the palladium monomer ([Pd(dppm)X_2]; X = Cl, Br, I) and dimer ([Pd_2(dppm)$_2X_2$]; X = Cl, Br, I) redistribution reactions display equilibrium constants close to the statistical value of 4.[67]

The activation parameters for the interconversion of **1**, **2**, and **3** have been calculated from the EXSY data and are summarized in Table 8. The large positive enthalpies of activation and the large negative entropies of activation are consistent with associative mechanistic pathways.[72−74] Calculation of the free energy of activation has allowed the determination of the relative energies for all of the reacting species (Figure 6). The relative thermodynamic stability of **2** with respect to **1** and **3** is readily apparent. The driving force for the reaction determined from Figure 6 is −1.0 kcal/mol. This is comparable and consistent with $\Delta G°$ calculated from the 1D spectra of −1.15 kcal/mol.

Mechanism. The mechanisms of redistribution reactions that have been studied in nonaqueous solvents have been shown to be associative in nature.[41,63,64,66,72]

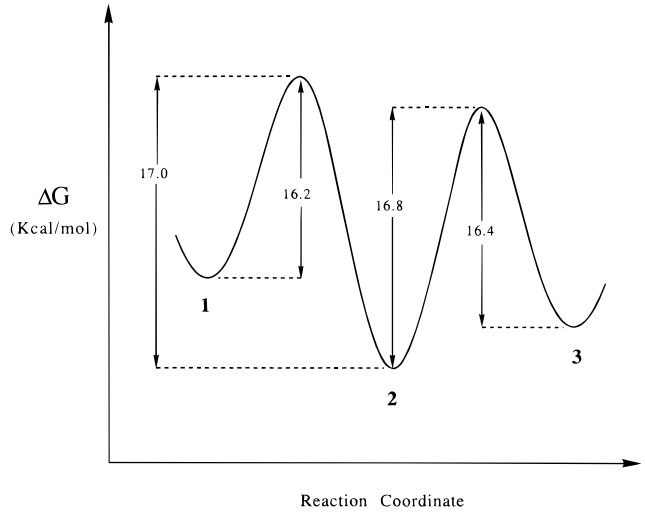

Figure 6. Proposed reaction coordinate for the interconversion of **1**, **2**, and **3**. Activation energies are in kcal/mol and are calculated from the rate data (30 °C) shown in Table 4.

A four-centered transition state is often postulated for redistribution reactions of main-group elements, which allows direct exchange of ligands.[41,54,58,59,61−65,67] We do not favor a four-centered transition state for this system, mostly due to the steric demands of the dppm ligand.

Square-planar d^8 complexes in general have been shown to react by associative mechanistic pathways for ligand substitution.[72−74] Solvent-assisted ligand dissociation has been studied extensively for the d^8 square-planar complexes of platinum and palladium.[72−74] These systems were studied in polar and nonpolar solvents where excess ligand was present. Ligand substitutions involving solvent assistance obey a two-term rate law (eq 8).[73,74] Thus, ligand substitution generally proceeds

$$\text{rate} = (k_s[\text{solvent}] + k_2[\text{Y}])[\text{complex}] \qquad (8)$$

$$k_s[\text{solvent}] = k_1$$

by two pathways. The first pathway (k_1) proceeds via

(71) Marcus, Y.; Eliezer, I. *J. Phys. Chem.* **1962**, *66*, 1661.
(72) Atwood, J. D. *Inorganic and Organometallic Reaction Mechanisms*; Brooks/Cole: Monterey, CA, 1985; Chapters 1 and 2, and references therein.
(73) Basolo, F.; Johnson, R. C. In *Coordination Chemistry*; Whitstable: Whitstable, U.K., 1986; pp 111−114.
(74) Langford, C. H.; Gray, H. B. In *Ligand Substitution Processes*; Karplus, R. B. a. M., Ed.; W. A. Benjamin: New York, 1965; pp 1−54.

solvent displacement, where species such as ML_3S^+ (S = solvent) are generated from a ML_3X complex.[73,74] The solvento species can then convert to the product where Y^- reacts with ML_3S^+, generating ML_3Y. A second pathway (k_2) exists where ML_3X can directly react with Y^-. In polar, coordinating solvents such as DMSO, the k_1 term dominates, since the addition of low concentrations of free ligand Y to a solution of **1** and **3** has little effect on the rate of exchange. In nonpolar, noncoordinating solvents such as methylene chloride and benzene the k_2 term dominates. Both pathways would give rise to negative activation entropies and positive activation enthalpies.[72,74] For the system **1**−**3**, coordination of DMSO followed by ligand displacement is implied by our results.[72−74] Scheme 1 presents a proposed mechanism for the conversion of **1** to **2**. A similar solvent-assisted pathway exists for conversion of **2** to **3**. Solvento intermediate species of the type depicted in Scheme 1 have not been observed by NMR, and conductivity studies of **1** in DMSO are consistent with a nonconducting solution. Since the concentration of NCS^- and/or Cl^- at any given time is expected to be exceedingly small, an associative interchange (I_a) mechanism pathway is proposed. Clearly the reaction rates in nonpolar, noncoordinating solvents such as methylene chloride and benzene are markedly slower, as indicated by the spectra shown in Figure 1. This is consistent with the solvent-assisted substitution processes. However, it is difficult to account for the fact that measurable rates of exchange still occur in benzene. Very inefficient (low k_s), but still viable, solvent substitution appears to be the most likely explanation, although catalysis by trace nucleophiles cannot be completely ruled out.

Conclusions

The halide/pseudohalide exchange between $Ni_2(dppm)_2(C{=}CH_2)(NCS)_2$ (**1**) and $Ni_2(dppm)_2(C{=}CH_2)Cl_2$ (**3**) has presented itself as a model system for analysis using the EXSY NMR technique. Two-dimensional EXSY NMR has proven to be a powerful and useful method for determining the forward and reverse rate constants and their respective exchange rates for systems at chemical equilibrium. Acquiring spectra at sufficiently short mixing times provides detailed mechanistic information that indicates which species are undergoing interconversion. Activation parameters can be determined which provide additional understanding of mechanistic pathways as well as the relative energetics of the reactants and products.

An interesting feature of this A-frame system is the enhanced stabilization of the mixed ligand species with respect to the two homogeneous halide and pseudohalide compounds, **3** and **1**, respectively. Our data are consistent with the two-term rate law typical of ligand substitution at d^8 square-planar metal centers. The mechanistic model that best describes terminal ligand redistribution for nickel A-frames is an associative interchange process. This assignment is made on the basis of the activation parameters, the relative rates in a number of different solvents, and the observed insensitivity of the rate to the addition of free ligand, at low concentrations.[74]

Acknowledgment. We gratefully acknowledge the National Science Foundation (Grant Nos. CHE-9319173 and CHE-9615886) for support. We thank Dr. Perry Pellechia and Dr. Dean Carlson for their helpful suggestions pertaining to this work.

OM980556J